



# Centrifuge Modeling of Soft Soil Reinforced with Granular Columns

Fernando Saboya · Sérgio Tibana · Rodrigo Martins Reis ·  
Thamara Fonte-Boa · Marcio de Souza Soares de Almeida · Maria Esther Soares Marques

Received: 23 August 2019 / Accepted: 13 December 2020 / Published online: 2 January 2021  
© The Author(s), under exclusive licence to Springer Nature Switzerland AG part of Springer Nature 2021

**Abstract** This paper presents a geotechnical centrifuge model of an embankment built in stages, over a 6.0 m layer of soft soil reinforced with nine floating granular columns arranged in a  $3 \times 3$  square grid. The container was divided in two compartments where reinforced and unreinforced soil were tested simultaneously for comparison purposes. The load was applied by means of a 4 m high sand embankment (prototype dimensions) built in three steps. For each step, the centrifuge was stopped to allow the placement of the embankment layer and then re-accelerated

up to 26 g and the excess of pore pressure was allowed to dissipate after each step. The instrumentation, comprised of total stress cells, pore pressure transducers and displacement transducers, was configured to collect information about the load transfer mechanism between the soil and the instrumented central column for each loading step during pore pressure dissipation. Results showed that despite representing only 30% of the total load, the first step provoked almost 70% of total vertical displacement. Finally, the columns were exhumed for a detailed and comprehensive visual analysis aiming to support and explain the results obtained.

---

F. Saboya (✉) · S. Tibana · R. M. Reis · T. Fonte-Boa  
Department of Civil Engineering, UENF,  
Campos Dos Goytacazes, RJ, Brazil  
e-mail: saboya@uenf.br

S. Tibana  
e-mail: tibana@uenf.br

R. M. Reis  
e-mail: reis@uenf.br

T. Fonte-Boa  
e-mail: thamara.fb@hotmail.com

M. S. S. de Almeida  
Graduate School of Engineering, Federal University of  
Rio de Janeiro, COPPE, Rio de Janeiro,  
RJ, Brazil  
e-mail: almeida@coc.ufrj.br

M. E. S. Marques  
Military Institute of Engineering - IME, Rio de Janeiro,  
RJ, Brazil  
e-mail: esther@ime.ed.br

**Keywords** Geotechnical centrifuge · Soil improvement · Physical modeling · Reinforced soil

## List of Symbols

$s_u$	Undrained shear strength
$\sigma'_v$	Effective vertical stress
OCR	Over consolidation ratio
$g$	Earth's gravity acceleration
$n$	Vertical stress concentration factor
$\Delta\sigma_{v(col)}$	Increment of vertical stress on the column
$\Delta\sigma_{v(soil)}$	Increment of vertical stress in the soil
$\beta$	Settlement reduction factor
$A_c$	Area of the column
$A_a$	Area of soil cell
$\Delta u$	Increment of excess of pore pressure
$e_0$	Initial void ratio

$e_{\min}$	Minimum void ratio
$e_{\max}$	Maximum void ratio
DR	Relative density
$D_{10}$	Equivalent 10% grain soil diameter passing by weight
$\phi_{\text{crit}}$	Critical shear strength friction angle
$c_c$	Compression index
$c_s$	Swelling index

## 1 Introduction

In the past several decades, numerous construction techniques have been proposed to improve the response of soft soil when submitted to embankment loading (Almeida and Marques 2013). One of the most common and widespread techniques is the installation of stone columns (granular piles) in the soft soil, which yields gains in stiffness and strength over time (Murugesan and Rajagopal 2010; Hu 1995; Almeida et al. 2014).

Das and Deb (2017) reported that a limited number of studies have been presented on stone column supported embankments and that most published results are related to analytical and numerical simulations of soil improvement (Abusharar et al. 2009; Borges et al. 2009; Indraratna et al. 2013; Basacket al. 2016; Rowe and Liu 2015; Das and Deb 2016, 2017). Reduced scale models have been used for studying the factors influencing the performance of reinforced embankments on soft soils, such as spacing, area replacement ratio, group effect, and aspect ratio, among other factors (Hughes and Withers 1974; Charles and Watts 1983; Bachus and Barksdale 1984; Narasimha Rao et al. 1992; Wood et al. 2000; McKelvey et al. 2004; Ambily and Gandhi 2007; Fattah et al. 2011). However, despite their important contributions, the majority of those tests were conducted in a 1 g environment, which does not reflect field conditions for stress level and scaling.

The performance of stone columns in ground improvement can be evaluated by means of several methods, including: analytical, numerical and physical. The latter, when conducted in a geotechnical centrifuge offers the advantage of replicating realistic scenarios including: stress state, time dependent stress-transfer mechanisms and loading history. Besides accelerating pore pressure dissipation, centrifuge modeling also has the advantage of well-identified

and, to some extent, controlled boundary conditions (Weber et al. 2010, 2006; Gautray et al. 2013).

The relative scarcity of centrifuge modeling studies of column-reinforced soil can be attributed to the complexities involved in such a modeling technique. Typically, for column installation at 1 g in reduced scale models, the sand, which simulates stone or gravel, is poured at the desired density inside of a previously driven tube that, in turn, is pulled out, as it is being filled (Almeida et al. 1985; Al-Khafaji and Craig 2000). Another installation process consists of freezing the sand columns, which are inserted in previously excavated shafts (Terashi et al. 1991; Kitazume et al. 1996; Rahman et al. 2000; Nakamura et al. 2006; Kimura 1983; Lee et al. 2001).

Lee et al. (2001) developed an equipment capable of installing columns at 1 g, using the soil displacement method. Further improvement to this device, carried out by Juneja (2002), Ng (2003) and Daramalinggam (2004) allowed for pile installation in-flight. In their studies, Lee et al. (2001) and Ng (2003) presented test results showing the influence of installation methods on the behavior of improved soil and concluded that the displacement method at 1 g and in-flight installation are better than the frozen pile method. The ideal is to install the columns in-flight in order to simulate actual prototype conditions, but this technique is complex and time consuming for a large group of columns (Ng et al. 1998).

This paper presents a geotechnical centrifuge model of a 4.0 m high prototype embankment over a 6.0 m thick layer of soft soil improved with nine stone columns arranged in a square grid. The displacement method for column installation was performed at 1 g and the model was then accelerated up to 26 g. The embankment was intentionally constructed in steps to allow for consolidation of the soft clay to occur at each step and enabling the assessment of the stress transfer mechanisms over time. Some centrifuge facilities are equipped with sand shower device to allow the construction of the embankment in-flight. Herein, for each step, the centrifuge was stopped for allowing the placement of embankment and, then, re-accelerated. It took around two minutes to reach the target of 26 times the Earth's gravity.

## 2 Experimental Procedure

The test was performed on the geotechnical beam centrifuge at the State University of Norte Fluminense, Rio de Janeiro, Brazil. The centrifuge, which has a 3.5 m radius and a 100 g-ton capacity, is capable of testing models of up to  $0.9 \times 0.9 \times 1.0$  m, weighing up to 1tf. Priebe (1995) has proposed an ideal area replacement of 10–30%, but values of 7.5% have been reported by Pires (2017). Although some authors (Shahu et al. 2000; Wood et al. 2000) have proposed that an area replacement above 25% is more efficient for this technique, the geometry used herein resulted in an area replacement ratio of 15.3%, which is approximately a typical stone column layout (Almeida et al., 2014). The experiment consisted of modeling an embankment constructed over a soft soil with nine columns equally distributed in a square grid and subjected to an acceleration of 26 g (Fig. 1). In the prototype, each 1.0 m diameter column was equally spaced at 2.27 m, attaining a clear span of 1.27 m. The length (L) of the columns was 5.35 m, yielding an L/D ratio of 5.35 which was suitable for developing full resistance and minimizing the possibility of lateral bulging (Hughes et al. 1975; Mitra and Chattopadhyay 1999; Bae et al. 2002; Black et al. 2007; Samadhiya et al. 2008; Najjar et al. 2010). The 4 m high prototype embankment was constructed applying dry sand material in three layers, in which the first layer was 1.25 m high and the other two were 0.75 m and 2.0 m

high respectively. The testing time between each embankment layer, during the centrifuge flight, was enough to allow for the consolidation of the soft soil and for the loading transfer mechanism to occur, as pointed out by the instrumentation installed in the model. The embankment sand in the model was placed in steps by means of a conventional sand pluviation to ensure homogeneity and an even surface. For each step, the centrifuge was stopped to allow the construction embankment layer. The total height of the embankment resulted in a vertical stress of approximately 56.4 kPa.

In order to compare the improved soil layer to an unimproved layer, an identical model, without columns, was built in a separate compartment of the same container. This unimproved model was constructed and tested in the same flight using the same soil and the same initial conditions.

### 2.1 Instrumentation

The model instrumentation shown in Fig. 2a–d comprised pore-pressure transducers, LVDTs and total stress cells. The Drucker PDC81 pore pressure transducers were placed on the two side walls of the container, in order to monitor the pore pressure development during consolidation and embankment loading. In addition, to measure settlements in the model with columns, two linear variable displacement transducers—LVDTs—were placed at the top of the

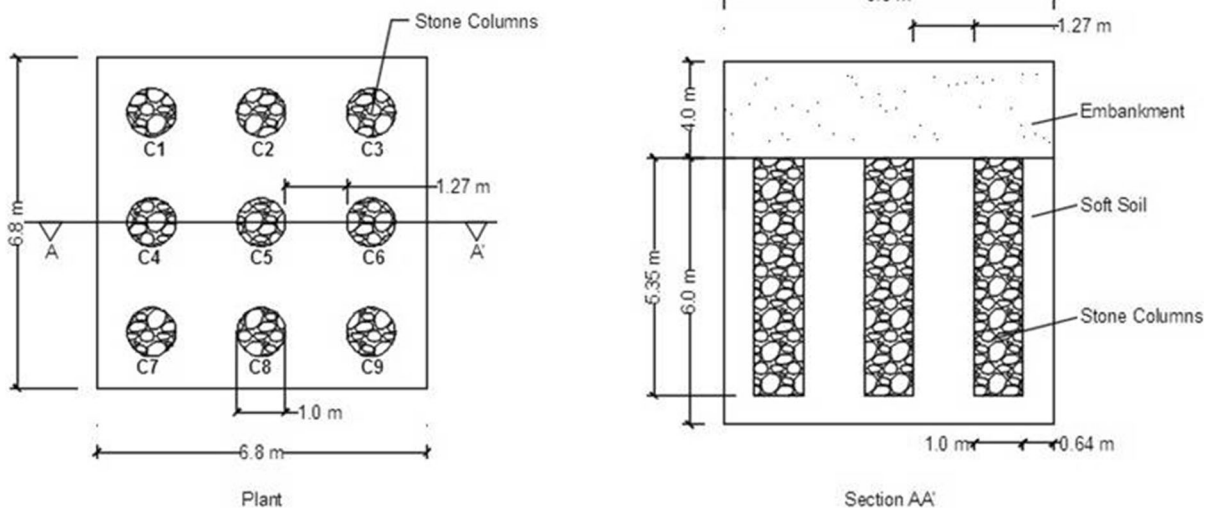


**Fig. 1** Case studied in prototype dimensions

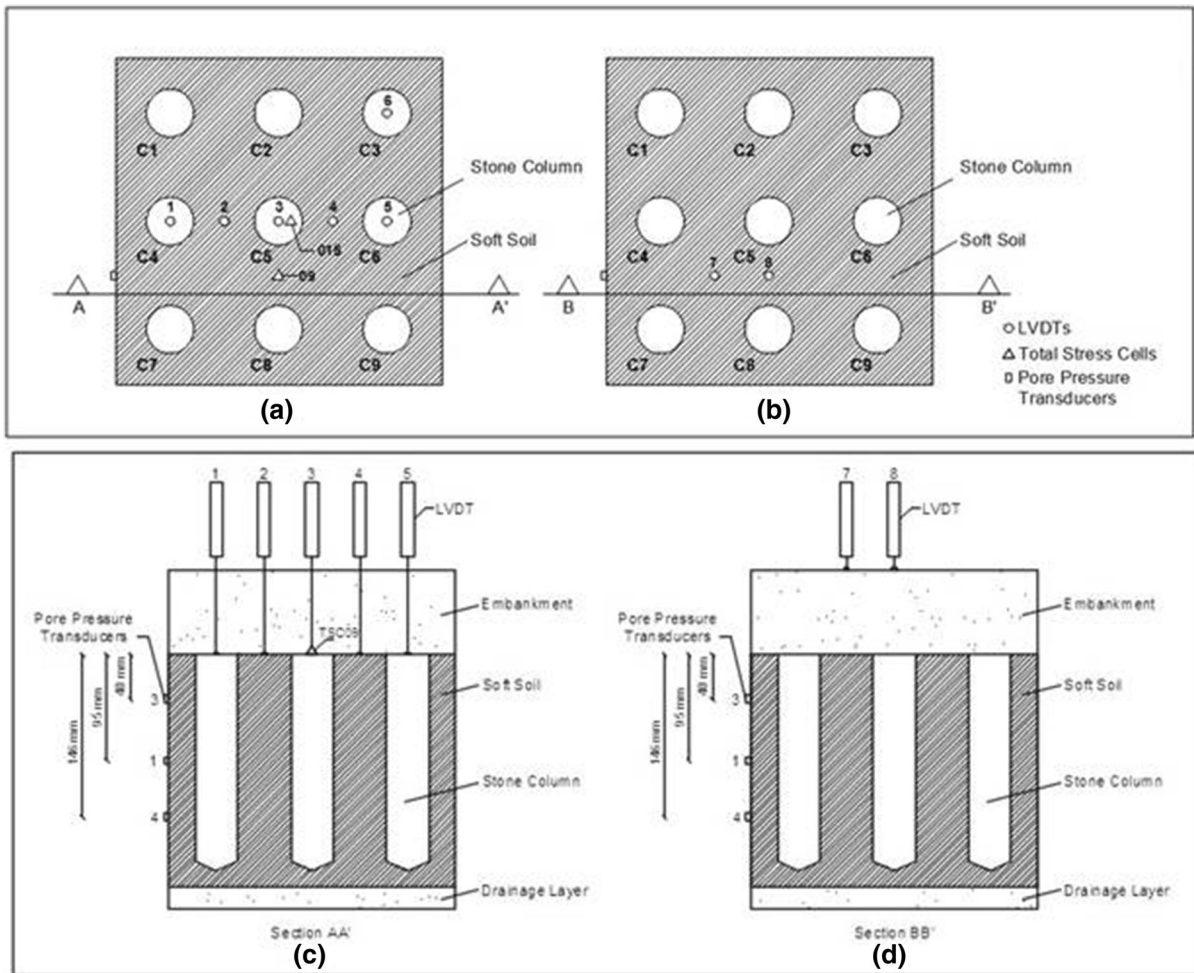


**Fig. 2** **a** Instruments at the base of the embankment; **b** instruments at the top of the embankment; **c** section AA' at the base of the embankment; **d** section BB' at the top of the embankment

clay soil, and four were placed directly on top of the columns (Fig. 2b). Two other LVDTs were placed on top of the sand embankment (Fig. 2c). These last needed to be relocated each time the centrifuge was stopped for the placement of a new sand layer.

Two ENTRAN EPL200-500SX mini total stress cells were used to monitor the load transfer in the model with columns during embankment construction and consolidation. One was placed at the top of the central column and the other was placed over the clay soil between two adjacent columns at the top of clay layer (at the contact between the clay and the sand embankment).

The calibration of all stress sensors was carried out in flight under a constant hydraulic head at different g-levels and they showed very consistent behavior.

## 2.2 Material Characterization, Consolidation Phase and T Bar Test

The soft soil was prepared from slurry chosen to adequately decrease the consolidation time in centrifuge flight. It is a mixture of kaolin (40%) and metakaolin (60%). The main geotechnical characteristics of this mixture are presented in Table 1 and the geotechnical characteristics of the materials used in the columns and the embankment are described in Table 2.

In general, as recommended by FHWA (1983), an undrained shear strength higher than 10–15 kPa is a minimum requirement for improving soft soil with stone columns without geosynthetic encasement. Therefore, in the first stage of centrifuge testing, at

**Table 1** Geotechnical characteristic of soil mixture

Material	Liquid limit (%)	Plastic limit (%)	Plastic index (%)	Specific gravity of soil particles	$c_c$	$c_s$	$c_c/(1 + e_o)$
Admixture (60% metakaolin + 40% kaolin)	59.3	29.0	30.4	2.54	0.29	0.029	0.107

**Table 2** Geotechnical characteristics of the sand used in the columns and in the embankment

Material	Specific gravity of soil particles	Minimum void ratio $e_{min}$	Maximum void ratio $e_{max}$	Relative density DR (%)	Void ratio $e$	Effective diameter $D_{10}(mm)$	Critical state friction angle ( $\phi_{crit}$ )
Column (sand)	2.64	1.42	1.66	70	1.49	0.3	33
Embankment (sand)	2.67	0.72	1.06	60	0.856	0.28	33

26 g, the aim was to obtain a soft soil with a minimum undrained shear strength ( $s_u$ ) within this range for the construction of the columns. The consolidation stages are described in Table 3.

The initial consolidation at 1 g (stage 1) was carried out to give the soil some strength in order to withstand the surcharge applied during the in-flight consolidation stages. Therefore, stage 2, which lasted a total of 7 h 40 min, consisted of consolidating the soil in flight at 26 g with a surcharge of 47.0 kPa, by the placement of weights on the soil, to achieve around 80% consolidation in the middle of the clay layer, reported by the pore pressure and settlement measured. This stage was controlled in order to follow the Cam-Clay relationship obtained from triaxial tests with this material (Eq. 1).

$$\frac{S_u}{\sigma'_v} = 0.27 \cdot OCR^{0.7} \tag{1}$$

At the end of this consolidation phase, the centrifuge was stopped, the surcharge weights (47 kPa) used in stage 2 were removed and a T-bar device was

quickly installed. The centrifuge was re-accelerated to 26 g and, after reconsolidation, the T-bar test was carried out in order to determine whether the strength would allow for construction of the columns. The resulting penetration rate yielded a normalized velocity greater than 100, as suggested by Randolph and Houlsby (1994), ensuring, thus, an undrained loading condition. The results showed a  $s_u$  with a mean value of 16 kPa at mid-height in the clay layer (Fig. 3). After the T-bar test was carried out, excess superficial water was drained and a 37.5 mm portion of the soil was trimmed to achieve a final layer thickness of 230 mm and the columns were immediately installed. It is important to mention that the portion of the soil surface removed was equivalent to approximately 15 kPa of vertical stress, which enabled the over consolidation ratio (OCR) value of 2.7 needed for attending Eq. 1. Figure 3 shows results before and after the complete consolidation caused by the embankment construction (discussed further ahead).

**Table 3** Summarizes all consolidation phases used to prepare the soil model

Consolidation phase	Gravity condition (g)	Applied vertical total stress (kPa)	Duration (h)
1	1	7.7	336
2	26	47.0	7.5

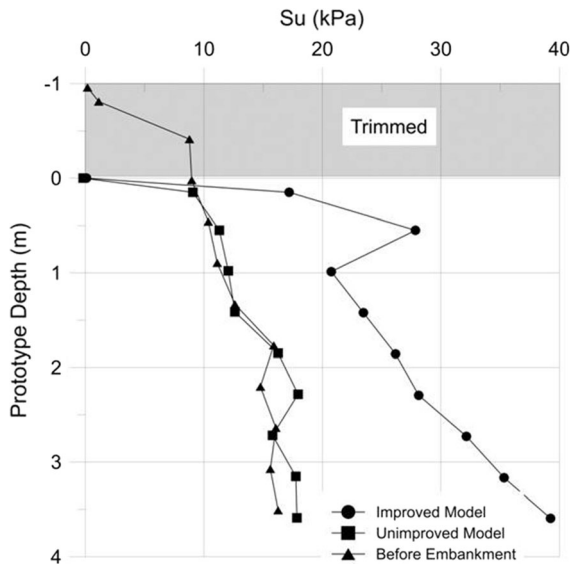


**Fig. 3** Undrained strength profiles of the model soft soil at the end of the test and before embankment construction

### 2.3 Installation of the Stone Columns

In order to assure the verticality of the columns, a special platform was used as a guide for holding the tubes during installation (Fig. 4). This platform consisted of a 50 mm thick polyurethane plate with nine 38 mm diameter holes, as shown in Fig. 4a. The guiding platform had a supporting structure, which allowed for the adjustment of the height inside the compartment. Nine aluminum tubes, inside of which sand was compacted with the aid of a tap hammer, were used for the column installation.

As a part of the driving process, a porous draining stone fabricated in the laboratory with a mixture of sand and epoxy was used. This porous stone was intentionally glued weakly to the tip of the tube with the objective of making the tube functioning as a closed-end pile during driving, in order to cause soil displacement during installation. The pore pressure generated during pile installation was not considered in the analysis because the model was, afterwards, consolidated during centrifuge flight.

The installation process is presented in details in Fig. 4b. The tube was driven into the soil by means of the guide platform until it reached the desired depth. Then the porous stone was pressed down lightly with the hammer tip in order to detach it from the end of the tube. The first amount of sand was subsequently

poured and compacted to the height corresponding to the target density, as the tube was gradually pulled out manually. This sequence continued until the entire column was installed. This procedure was then repeated for all of the remaining columns.

At the top of the soft soil, two total stress cells and the circular pads for supporting the LVDT rods were installed according to the instrumentation plan. For the LVDTs that cross the embankment, thin outer open tubes were used to reduce friction and enable free displacement of the rods.

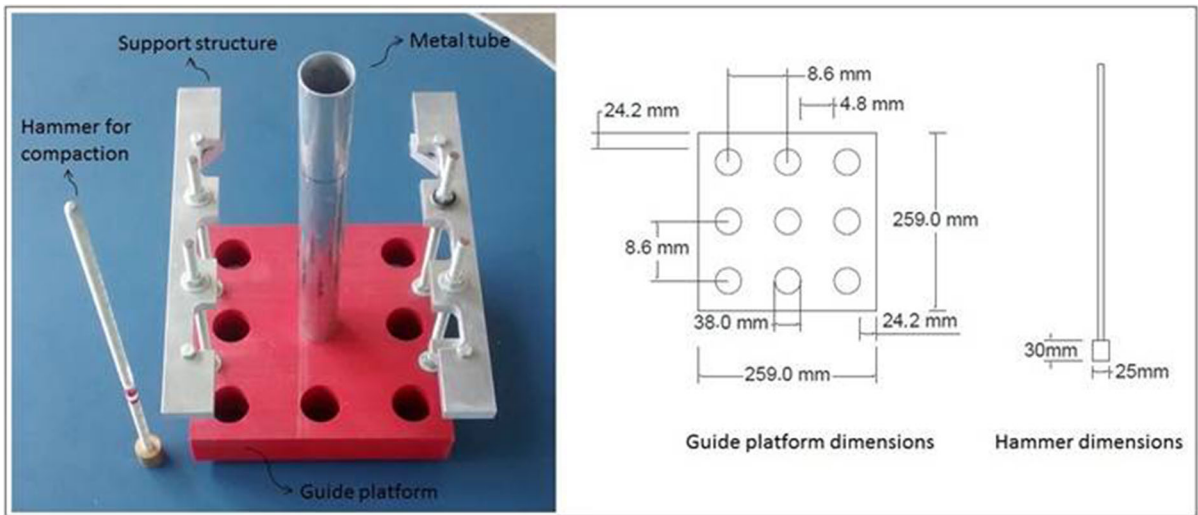
### 2.4 Embankment Construction

The first sand embankment layer of 47.5 mm was applied using a calibrated sand-shower to obtain the required density. This layer corresponds to a surcharge of 17.6 kPa. After the placement of the first embankment layer, the LVDTs were installed with a special acrylic support. For displacement measurements at the top of clay layer, a LVDT with prolonged rod was inserted into the sand layer built in this first step, and carefully positioned over the small circular aluminum pads that had been previously placed between the two layers.

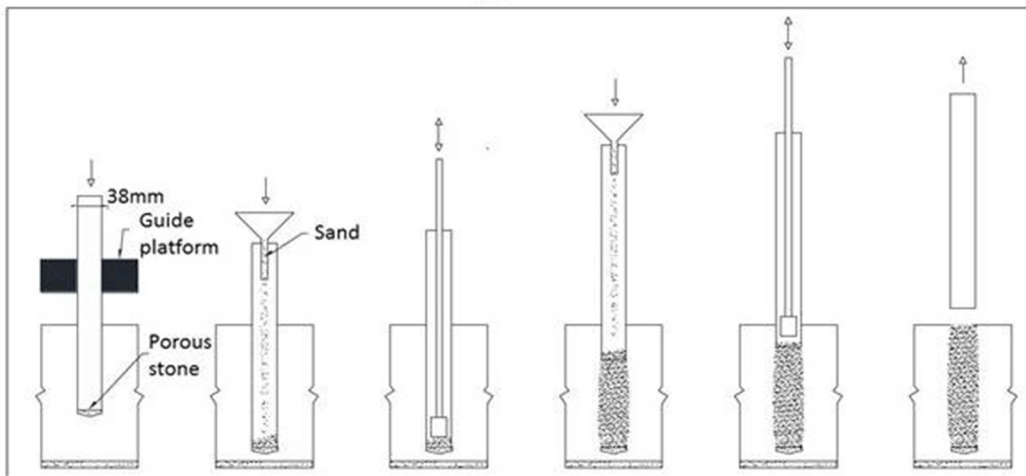
To initiate the construction of the second embankment layer, the centrifuge was stopped and the LVDT supporting device was disassembled and repositioned. Afterward, the centrifuge was re-accelerated up to 26 g. The second embankment layer represents an increment of 10.6 kPa, totaling 28.2 kPa of surcharge. The same procedure was used for the third embankment layer. Table 4 shows details of all the embankment construction stages.

It is important to mention that this procedure has some shortcomings regarding the stress history during spin-down and spin-up of the centrifuge for each step. However, the placement of each step lasted less than five minutes and the re-acceleration took two minutes to reach the desired g-level. Therefore, the unwanted effects were kept minimum regarding changes in the stress history of the model.

After the end of the test, the model was again accelerated to restore the effective stress and two T-bar tests were carried out in-flight. One test was conducted in the compartment of the unimproved soil, where the first T-bar test had already been done after the consolidation phase, and the other in the improved soil between two adjacent columns. Both clay layers



(a)



(b)

**Fig. 4** a Tools used to install the stone columns, b process used for installation stone columns

**Table 4** Loading scheme in both improved and unimproved models

Loading stage	Embankment's prototype total thickness (m)	Total vertical stress (kPa)	Increment of vertical stress (kPa)
1	1.25	17.63	17.63
2	2.00	28.2	10.57
3	4.00	56.4	28.2

showed an increase in undrained shear strength relative to depth, as expected, but the gain in undrained strength for the improved model was substantially higher than the unimproved one, as seen in Fig. 3.

### 3 Results

#### 3.1 Settlements and Excess Pore Pressure

The initial excess pore pressure, normalized to the vertical total stress increment resulting from the

placement of each sand layer (each step), is shown in Fig. 5 for different depths. In the model, the excess pore pressure corresponds to the maximum centrifuge acceleration after construction of each layer, considering that no drainage took place in this period of re-acceleration that lasted around two minutes to get back to 26 g level. The increase in the pore pressure after the placement of the first layer and after reaching the centrifuge acceleration of 26 g varies from 0.92 to 0.85 for the model with columns. Equally, for the second and the third loading stages, following the same test procedure of the first step, pore pressure generation drops considerably for the model with columns and remains higher than 0.85 for the model without columns. Since the increment of vertical stress inside the soil was not measured, the pore pressure ratio, as shown in Fig. 5, provides an indication of the overall performance of the improved model, i.e., subsequent lower values of the pore pressure ratio suggest that the column stress transfer mechanism is taking place, otherwise the ratio would be close to unity and all stresses imposed by the newly added embankment layer would be reflected in the pore pressure increment. Similar behavior has been reported based on field studies (Almeida et al. 2014; Lima et al. 2019).

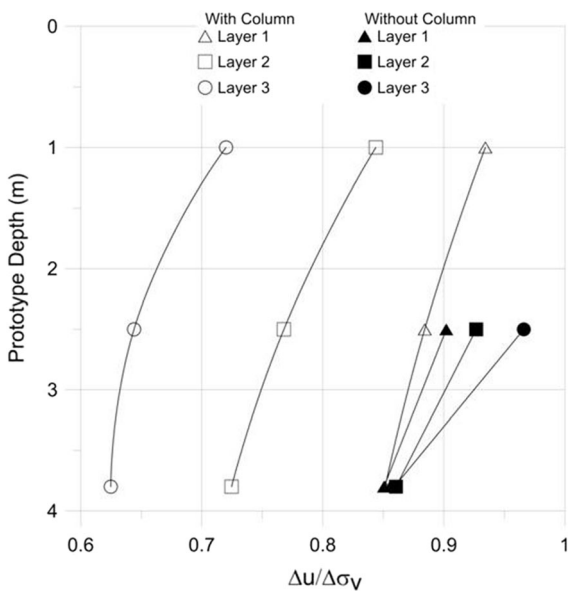


**Fig. 5** Initial excess of pore pressure with prototype depth after placement of each layer

In the model without columns, as expected, pore pressure ratios close to unity were observed, indicating a behavior typical of unimproved undrained soft soil, where the total stress increment is mostly transferred to the pore fluid. Figure 5 allows for a direct comparison of the benefits of the columns and the construction in stages adopted in this study. Waiting for the consolidation after the preceding layer is placed appears to be a good strategy for reducing the generation of pore pressure for the subsequent loads, once the stress transfer mechanism is initiated during the placement of the first embankment layer. Figure 5 shows that the pore pressure ratio decreased from 0.94 to 0.72 at a depth of 1.0 m, during time interval from the placement of embankment layer 1 to layer 3. The high pore pressure ratio for the first load is consistent with the low arching effects for thin embankment. In contrast, for the unreinforced soil the pore pressure ratio increases with the embankment load.

Figure 6 illustrates a cross section of the model, showing that approximately 70% of total settlement occurred after the placement of the first layer, despite the fact that this layer represents only 30% of the embankment height. The settlement profile shown in Fig. 6 suggests that central column suffered a drag-down process due to the settlement of the soil around

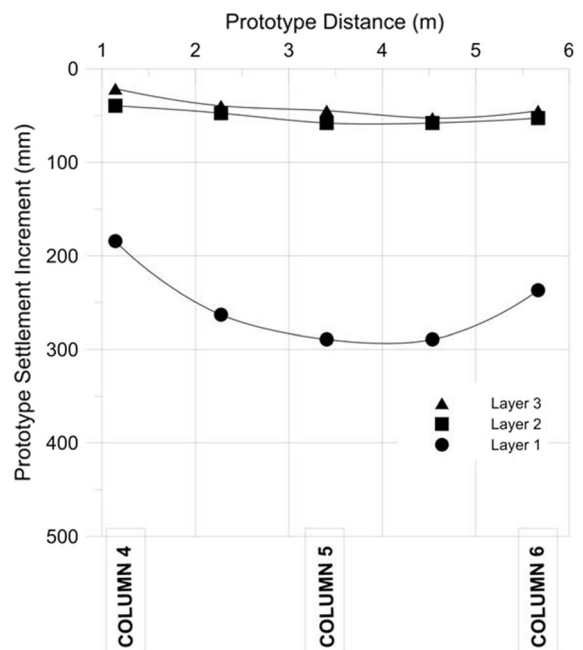


**Fig. 6** Settlements at the embankment base following placement of each embankment layer (stage)



it, which absorbed the load increment from the first embankment layer and, therefore, due to lack of good soil support, showed high settlement increment. As a result of the consolidation caused by the placement of the first surcharge, the soil became stiffer and gained enough strength to display satisfactory behavior under the second and third load increments, which represented 70% of total load and were responsible for only 30% of the total settlement. It is important to mention that the final layer represented 50% of total vertical load increment.

### 3.2 Load Transfer

In order to measure the vertical stress transfer in the central column and surrounding soil, a total stress cell was placed on the top of the column. Another cell was installed at the soil-embankment interface, mid-distance between two adjacent columns. These two total stress cells are shown in Fig. 7a. The reference initial stresses were measured just after the centrifuge reached the required acceleration for each embankment layer.

The vertical stresses at the top of the central column and in the surrounding soil, after the placement of the first layer, are presented in Fig. 7a. Immediately after the centrifuge reached the planned acceleration, both cells showed the same results (approx. 20 kPa). However, this was followed by a drop in the vertical

stress in the pile, indicating that the pile suffered considerable settlement resulting from a possible dragdown effect, reducing, temporarily, the vertical stress over it. Soon after this initial event, the vertical stress transfer began, as evidenced by a marked stress decrease in the soil, concurrent with an increase in stress in the pile head. Stabilization was observed 30 min (centrifuge time) or 14 days (prototype time) after layer placement. It is notable that the first layer of 1.25 m (prototype scale) was not high enough to fully develop the arching effect (Yun-min et al. 2008), and, therefore it played the role of provoking the consolidation of the soil in order to better support the subsequent loads increments.

As a result of this process, a different response was observed during the second and third layer placements, as illustrated in Fig. 7a, b. From the beginning of the loading, the vertical stress in the pile was, as expected, always greater than that in the soil, indicating an efficient stress transfer mechanism. This response shows that the first layer not only provided a more uniform distribution of the load increment over the affected area, but also, a reasonable initial bearing support. This mechanism is closely linked to the fact that, after the end of first layer placement, 70% of the total settlement had already occurred, as already mentioned. On the other hand, the difference between the vertical stress supported by the column and the one

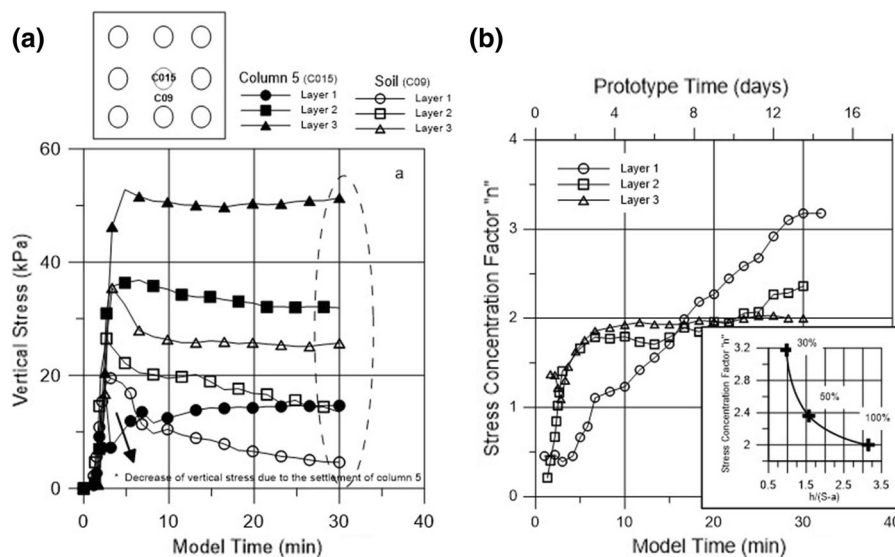


**Fig. 7** a Evolution of vertical stresses with the time after the construction of each layer. b Resulting stress concentration factor

transmitted to the soil, increases as the height of embankment increases.

Equation 2 can be used to define the stress concentration factor  $n$  which expresses the ratio between the mean vertical stress in the column and the surrounding soil. The  $n$  factor at the end of the stress transfer should be understood as the load transfer after the consolidation for each loading phase. It is possible to observe this stress transfer effect resulting from the placement of each layer, as shown in Fig. 7b, expressing the stress concentration factor with the progress of the embankment construction.

$$n = \frac{\Delta\sigma'_v(\text{col})}{\Delta\sigma'_v(\text{soil})} \quad (2)$$

With the stress concentration factor  $n$ , it is possible to determine the theoretical settlement reduction factor,  $\beta$ , defined as (Almeida and Marques 2013):

$$\beta = 1 + (n - 1) \cdot \frac{A_c}{A} \quad (3)$$

This factor expresses the rigidity or the capability of the embankment to sustain or transmit the stress to the columns. Contrary to the expectation for one-step loading, the stress concentration factor drops as the embankment rises. This is closely related to the construction of the embankment in stages instead of being placed in one single step, allowing for pore pressure dissipation with a consequent increase in soft soil effective stress that is enough to support the subsequent loads.

Taking into account that the stress concentration factor  $n$  (Eq. 2) varies with the incremental layers of the embankment as shown in Fig. 7b, the values of the theoretical settlement reduction factor,  $\beta$  (Eq. 3) obtained for each layer placement, after stabilization of the loading transfer mechanism, decrease from 1.35 to 1.15 (Fig. 8).

According to Priebe's theory (Priebe 1995), the  $33^\circ$  friction angle of the sand column in the present study (Santiago 2010) would call for a theoretical settlement reduction factor of 1.2. However, the results reported in this study should not be adjusted to Priebe's prediction for the subsequent loads, because it was originally developed for end bearing stone columns.

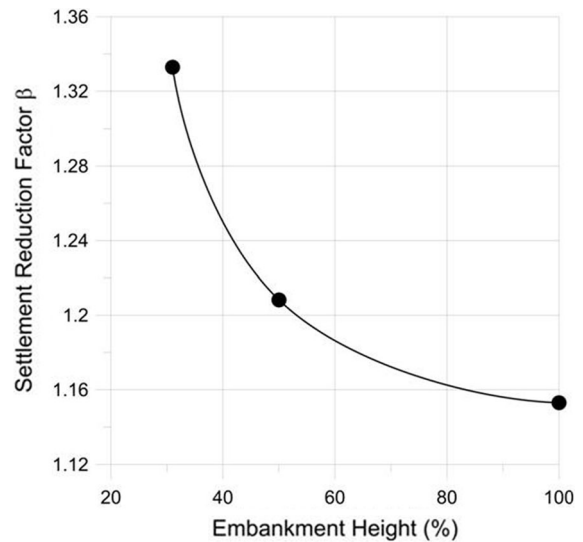


**Fig. 8** Relation between the settlement reduction factor and the percentage of embankment constructed

### 3.3 Model Exhumation

In order to search for an explanation for some of the observed results registered by the instruments, the columns were exhumed. The container was disassembled and the model was carefully trimmed to expose the columns. Figure 9 shows the first row of columns 7, 8 and 9, where some of the shortcomings of the construction method are evident. The tips of columns 8 and 9 deviated from verticality. This deviation probably occurred during the extraction of the tube when the pressure exerted by the compaction rod over the stone tip was, in some way, not strong enough to detach it completely from the tube tip. So, during the extraction, part of the stone may still have been glued to some points of the tube tip.

This problem which occurred in columns 8 and 9 was repeated in other columns in the model and it appears even more pronounced in column 5 and column 2 (Fig. 10). It is important to mention that column 5 was located at the center of the model where most attention was paid and most of the analyses were concentrated. On the other hand, the totality of the columns appear to be in good structural conditions without any signal of bulging, failure or discontinuity.

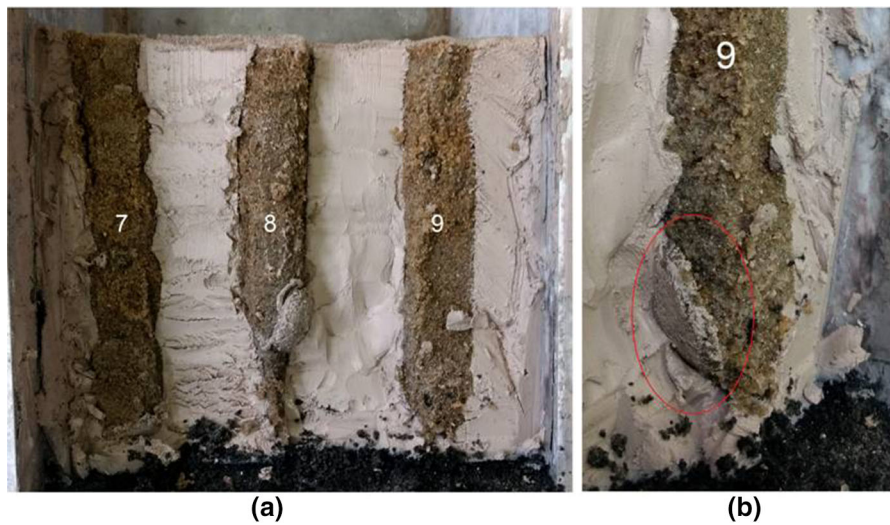


**Fig. 9** Front view of columns 7, 8 and 9 after exhumation and detail of the bulged draining stone of column 9



**Fig. 10** Exhumation of columns 4, 5 and 6

#### 4 Conclusions

Geotechnical centrifuge modeling is a powerful tool for investigating the inherent characteristics of complex problems such as soil reinforcement. A direct and simultaneous comparison between improved and unimproved soft soil was possible by using two models with equal embankment heights in the same centrifuge box running at the same time.

Floating stone columns can display satisfactory behavior as well, as long as the embankment is built in stages and the load transfer mechanism is fully restored overtime. This finding indicates that a layer placement plan that includes an adequate time interval between layers, allowing pore pressure to dissipate, is a procedure, which merits further investigation. In this study, the last two load increments (layer 2 and 3) were responsible for 70% of the total load, however, they accounted for only 30% of the total settlement. This behavior has been attributed to the settlement of the columns and the progressive consolidation of the soft soil during the loading in steps. Under the last two embankment steps, the treatment showed higher efficiency where smaller settlements were observed. This, particularly, enabled the evaluation of the behavior of the columns and their performance as a soft soil improvement technique when the load is applied in steps.

The overall performance of the treatment was assessed with T-bar tests that showed, as expected, an increase in strength in comparison with unimproved model. This was also confirmed by the increase in pore pressure with increasing depth for each construction step, where the improved soil presented low values for the second and third embankment increment, suggesting that the soft soil rapidly gained strength and stiffness after the first step, along with the development of a stress transfer mechanism.

In general, the results demonstrate the benefits of the columns, with an emphasis on consolidation time and the stress concentration. The stress transfer mechanism was found to depend on the advancement of the embankment layers. Furthermore, the settlement depends on the time between two consecutive loading steps. The response of the stress distribution during the loading progress was found to be important for evaluating the efficiency of columns as a rigid inclusion.

**Acknowledgements** The Authors are grateful to Rio de Janeiro Research Agency FAPERJ and Federal Scholarship Agency CAPES for funding this research.

**Funding** Fundação Carlos Chagas Filho de Amparo à Pesquisa do Estado do Rio de Janeiro (Grant No. 101.240/2014).

#### Compliance with ethical standards

**Conflict of interest** The Authors declare that this manuscript has no conflict of interest and that the data from the tests presented herein are available in <http://uenf.br/posgraduacao/engenharia-civil/dissertacoes-de-mestrado/>.

#### References

- Abusharar SW, Zheng JJ, Chen BG, Yin JH (2009) A simplified method for analysis of a piled embankment reinforced with geosynthetics. *Geotext Geomembr* 27(1):35–52
- Al-Khafaji ZA, Craig WH (2000) Drainage and reinforcement of soft clay tank foundation by sand columns. *Geotechnique* 50(6):709–713
- Almeida MSS, Marques MES (2013) Design and performance of embankments on very soft soils. CRC Press, Boca Raton
- Almeida MSS, Davies MCR, Parry RHG (1985) Centrifuge tests on embankments on strengthened and unstrengthened clay foundations. *Geotechnique* 35(4):425–441
- Almeida MSS, Lima B, Riccio M, Jud H, Cascao M, Roza F (2014) Stone columns field test: monitoring data and numerical analyses. *Geotech Eng J SEAGS AGSSEA* 45(1):103–112
- Ambily AP, Gandhi SR, Shailesh R (2007) Behavior of stone columns based on experimental and FEM analysis. *J Geotech Geoenviron Eng ASCE* 133(4):405–415
- Basack S, Indraratna B, Rujikiatkamjorn C (2016) Modelling the performance of stone column reinforced soft ground under static and cyclic loads. *J Geotech Geoenviron Eng ASCE* 142(2):04015067-1-04015067-15
- Babu MRD, Nayak R, Shivashanka R (2013) A critical review of construction, analysis and behaviour of stone columns. *Geotech Geol Eng* 31:1–22. <https://doi.org/10.1007/s10706-012-9555-9>
- Bae WS, Shin BW, An BC (2002) Behavior of foundation system improved with stone columns. In: Proceedings 12th international offshore and polar engineering. Conference, Kitakyushu, Japan, pp 675–678
- Bachus RC, Barksdale RD (1984) Vertical and lateral behaviour of model stone columns. In: Proceedings of the international conference on in situ soil and rock reinforcement, Paris, pp 99–104
- Black JA, Sivakumar V, Madhav MR, Hamill GA (2007) Reinforced stone columns in weak deposits: laboratory model study. *J Geotech Geoenviron Eng ASCE* 133(9):1154–1161
- Borges JL, Domingues TS, Cardoso AS (2009) Embankments on soft soil reinforced with stone columns: numerical analysis and proposal of a new design method. *Geotech Geol Eng* 27(6):667–679
- Charles JA, Watts KA (1983) Compressibility of soft clay reinforced with granular columns. In: Proceedings of the 8th European conference on soil mechanics and foundation engineering, Helsinki, pp 347–352
- Daramalinggam JAL (2004) Bearing capacity of clay bed improved by sand compaction piles under caisson loading. MSc Thesis, Singapore, National University of Singapore – NUS, 186p
- Das AK, Deb K (2016) Response of cylindrical storage tank foundation resting on tensionless stone column-improved soil. *Int J Geomech ASCE*. [https://doi.org/10.1061/\(ASCE\)GM.1943-5622.0000697](https://doi.org/10.1061/(ASCE)GM.1943-5622.0000697)
- Das AK, Deb K (2017) Modeling of stone column-supported embankment under axi-symmetric condition. *Geotech Geol Eng* 35:707–730. <https://doi.org/10.1007/s10706-016-0136-1>
- Deb K (2010) A mathematical model to study the soil arching effect in stone column-supported embankment resting on soft soil. *Appl Math Modell* 34(12):3871–3883
- Deb K, Basudhar PK, Chandra S (2010) Axi-symmetric analysis of geosynthetic-reinforced granular fill-soft soil system with group of stone columns. *Geotech Geol Eng* 28(2):177–186
- Fattah MY, Shlash KT, Al-Waily MJM (2011) Stress concentration ratio of model stone columns in soft clays. *Geotech Test J ASTM* 34(1):1–11
- FHWA (1983) Design and construction of stone columns, vol 1. Report FHWA/RD-83/027, Barksdale RD, Bachus RC (eds), Federal Highway Administration
- Gautray J, Laue J, Springman SM, Almeida MSS (2013) Development of pore water pressure around a stone column. In Proceedings of the 18th international conference on soil mechanics and geotechnical engineering, Paris, France, pp 1–5
- Hu W (1995) Physical modelling of group behaviour of stone column foundations. D.Sc. Thesis, Glasgow University, Scotland, p 312
- Hughes JMO, Withers NJ (1974) Reinforcing of soft cohesive soils with stone columns. *Ground Eng* 7(3):42–49
- Hughes JMO, Withers NJ, Greenwood DA (1975) Afield trial of the reinforcing effect of a stone column in soil. *Geotechnique* 25(1):31–44
- Iai S (1988) Large scale model tests and analysis of gravel drains. Report of the Port and Harbor Research Institute 27(3), Japan
- Indraratna B, Basack S, Rujikiatkamjorn C (2013) A numerical solution of stone column improved soft soil considering

- arching, clogging and smear effects. *J Geotech Geoenviron Eng* 139(3):377–394
- Juneja A (2002) Centrifuge model study of the effects of sand compaction pile installation on soft clay ground. Ph.D. Thesis, National University of Singapore
- Kimura, T (1983) Centrifuge tests on sand compaction piles. In: Proceedings of the seventh Asian regional conference on soil mechanics and foundation engineering, Haifa—Israel, pp 255–260
- Kitazume M, Miyajima S, Nishida Y (1996) Stability of re-vestment on soft clay improved by SCP. In: Proceedings of the second international conference on soft soil engineering, Nanjing—China, vol 2, pp 455–460
- Lee FH, Ng YW, Yong KY (2001) Effects of installation method on sand compaction piles in clay in the centrifuge. *Geotech Test J* 24(3):314–323
- Lima BT, Almeida MSS, Hosseinpour I (2019) Field measured and simulated performance of a stone columns-strengthened soft clay deposit. *Int J Geotech Eng*. <https://doi.org/10.1080/19386362.2019.1653506>
- Lima BT (2012) Study on the use of stone columns in very soft soil clays. D.Sc. Thesis, COPPE/UFRJ, Rio de Janeiro, Brazil, p 321 (in portuguese)
- McKelvey D, Sivakumar V, Bell A, Graham J (2004) Modeling vibrated stone columns in soft clay. *Proc Inst Civ Eng Geotech Eng* 157(3):137–149
- Mitra S, Chattopadhyay BC (1999) Stone columns and design limitations. In: Proceedings, Indian geotechnical conference, Calcutta, India, pp 201–205
- Murugesan S, Rajagopal K (2010) Studies on the behavior of single and group of geosynthetic encased stone columns. *J Geotech Geoenviron Eng ASCE* 136(1):129–139
- Najjar SS, Sadek S, Maakaroun T (2010) Effect of sand columns on the undrained load response of soft clays. *J Geotech Geoenviron Eng ASCE* 136(9):1263–1277
- Nakamura T, Kitazume M, Takahashi H (2006) Centrifugal model tests and numerical calculations on failure pattern of floating type SCP improved ground. In: Proceedings of geo Shanghai international conference, Shanghai—China, pp 119–126
- Narasimha Rao S, Prasad YVS, Hanumanta Rao V (1992) Use of stone columns in soft marine clays. In: Proceedings of the 45th Canadian geotechnical conference, Toronto, Ont, October, p 1–9
- Ng YW (2003) Centrifuge modelling of the installation of sand compaction piles in soft clay. PhD thesis, National University of Singapore
- Ng YW, Lee FH, Yong KY (1998) Development of an in-flight Sand Compaction Pile (SCP) installer. In: Proceedings of the international conference centrifuge, 98, Tokyo—Japan, pp 837–844
- Pires LGS (2017) Comportamento de Aterro Experimental Sobre Solo Mole Tratado com Colunas De Brita. MSc Dissertation, COPPE/UFRJ, Rio de Janeiro, Brazil, p 143 (in portuguese)
- Priebe HJ (1995) The design of vibro replacement. *Ground Eng* 28(10).
- Rahman Z, Takemura J, Kouda M, Yasumoto K (2000) Experimental study on deformation of soft clay improved by low replacement ratio SCP under backfilled caisson loading. *Soils Found* 40(5):19–35
- Randolph MF, Houlsby GT (1994) T-bar penetration testing in soft clay. *J Geotech Eng* 120(12):2230–2235
- Rowe RK, Liu K-W (2015) Three-dimensional finite element modelling of a full-scale geosynthetic-reinforced, pile-supported embankment. *Can Geotech J* 52(12):2041–2054
- Samadhiya NK, Maheswari P, Basu P, Kumar MB (2008) Load settlement characteristics of granular piles with randomly mixed fibres. *Indian Geotech J* 38(3):345–354
- Santiago PAC (2010) Experimental study of buried pipes under pullout load using geotechnical. MSc Dissertation, State University of Norte Fluminense Darcy Ribeiro – UENF, Rio de Janeiro, Brazil, 101p (In Portuguese)
- Sasaki Y, Taniguchi E (1982) Shaking table on gravel drains to prevent liquefaction of sand deposits. *Soils Found* 22(3):1–14
- Shahu JT, Madhav MR, Hayashi S (2000) Analysis of soft ground—granular pile-granular mat system. *J Comput Geotech* 27(1):45–62
- Terashi M, Kitazume M, Okada H (1991) Applicability of practical formula for bearing capacity of clay improved by SCP. In: Proceedings of the international conference on geotechnical engineering for coastal development: theory and practice on soft ground, Yokohama—Japan, vol 1, pp 405–410
- Yun-min C, Wei-ping C, Ren-peng C (2008) An experimental investigation of soil arching within basal reinforced and unreinforced piles embankments. *Geotext. Geomembr* 26(2):164–174
- Weber TM, Plotze M, Laue J, Peschke G, Springman SM (2010) Smear zone identification and soil properties around stone columns constructed in-flight in centrifuge model tests. *Geotechnique* 60(3):197–206. <https://doi.org/10.1680/geot.8.P.098>
- Weber TM, Laue J, Springman S (2006). Centrifuge modelling of sand compaction piles in soft clay under embankment load. In: Proceedings of the 6th international conference on physical modelling in geotechnics, Hong-Kong, pp 1–6
- Wood DM, Hu W, Nash DFT (2000) Group effects in stone column foundations: model tests. *Geotechnique* 50(6):689–698

**Publisher's Note** Springer Nature remains neutral with regard to jurisdictional claims in published maps and institutional affiliations.